2018 IEEE/RSJ International Conference on Intelligent Robots and Systems (IROS)
Madrid, Spain, October 1-5, 2018

Interspecies Retargeting of Homologous Body Posture Based on Skeletal Morphing

Ko Ayusawa[1], Yosuke Ikegami[2], Akihiko Murai[3], Yusuke Yoshiyasu[1],
Eiichi Yoshida[1], Satoshi Oota[4] and Yoshihiko Nakamura[3]

Abstract— **The paper aims to develop a methodology of transferring the knowledge obtained from the experiments of laboratory animals to human musculoskeletal system. To achieve the goal, we propose a method for estimating the homologous posture of the mammalian skeletal system corresponding to the human body posture. We hypothesize the homology of bone geometry between mammalian species implies that of biomechanical functions. The method relies on this homology and determines the homologous postures according to the anatomical landmarks of bone geometry. This paper shows the results of the analysis on homologous postures between the human and mouse skeletal models to validate our hypothesis. A pilot study also introduces comparison of mechanical functions between the two models by using the homologous postures.**

I. INTRODUCTION

The technology of motion analysis can provide various information and insights about the dexterous human movement generated by the complex interaction between human body functions such as bones, muscles, and neural systems. The knowledge about those functions realizing human movements is useful not only in medical or biomechanical fields but also for robotics applications, in order to design body structure and control system for robots. Meanwhile, the robotics technologies of modeling, control, and simulation have been applied to human motion analysis and simulation [1]. In recent days, the detailed human musculoskeletal models have been developed [1], [2], which enables the reconstruction of joint movements as well as the estimation of human muscle activities during movements [3]. The analysis with such sophisticated human models, however, suffers from various unknown parameters in the computational models of muscles and neural systems. This is because some parameters in the muscular or neural models are difficult to be measured by human subject experiments and often estimated indirectly by simulation [4]. Another difficulty lies in the need of the experimental validation when evaluating the accuracy of the estimated models.

Technologies to analyze human movements such as motion capture can also be applied to the other mammalian animals. In general, the experimental data using animals can provide important information which cannot be obtained from human experiments. Mice are especially useful laboratory animals for biomedical studies because of the low cost of breeding and the recent advancement of genetic modification techniques. They are known to have a close biological relationship with humans. The two species share a common genome and show homology in their phenotypes [5], making mice important as laboratory animals. Mouse genome information is also available in public databases [6]. The methodology to transfer the biological knowledge obtained from laboratory mice to humans is considered as a useful tool to study the genetic disorders. Such knowledge usually comes from the observation at the cellular level or macroscopic level such as social behaviors. If the knowledge obtained from biomechanical analysis of laboratory mice can be transferred to the knowledge for humans, it will be an important clue to evaluate the validity of the methodology of neuromusculoskeletal analysis and simulation.

This paper ambitiously aims to transfer the neuromusculoskeletal knowledge between the two species. First of all, musculoskeletal modeling of a mouse is essential to analyze its movements. While there are some literatures on the skeletal system of mouse [7], there are few works on modeling of musculotendinous system [8], [9]. CT and MRI images are important sources of anatomical information of musculoskeletal system. However, the resolution of MRI imaging is usually not enough for small laboratory mice. Though X-ray CT scanning is useful when scanning skeletal system in detail, it remains a technical difficulty in obtaining the placement of muscles. Some researchers reported the musculoskeletal analysis of laboratory animals such as rats [10] or mouse [8], [9], there still remains the problem of modeling the whole body musculoskeletal system. Since our goal is to transfer the experimental information of laboratory animals to the human, a new framework is also necessary for the correspondence between the human model and the mammalian model.

Our previous work proposed a systematic method for building a musculoskeletal model of a mammalian animal, specifically of a laboratory mouse [11]. The method called ”musculoskeletal morphing” can map the musculotendinous location of the whole-body human musculoskeletal model [1] onto the mouse skeletal model reconstructed by X-ray CT scanning [12]. The musculoskeletal morphing relies on the homology of bone geometry between mammalian species. The method designs a geometrical morphing map from one

---

[1] K. Ayusawa, Y. Yoshiyasu and E. Yoshida are with CNRS-AIST JRL (Joint Robotics Laboratory), UMI3218/RL, Intelligent Systems Research Institute, National Institute of Advanced Industrial Science and Technology, Japan. `{k.ayusawa, yusuke-yoshiyasu, e.yoshida}@aist.go.jp`

[2] Y. Ikegami and Y. Nakamura are with the Department of Mechano-Informatics, University of Tokyo, Japan.

[3] A. Murai is with Human Informatics Research Institute, National Institute of Advanced Industrial Science and Technology, Japan.

[4] S. Oota is with BioResource Center, RIKEN, Japan.

978-1-5386-8093-3/18/$31.00 ©2018 IEEE

bone of the human skeletal system to the corresponding one of the other mammalian skeletal system. The muscular geometrical information such as muscle attachment points can be transferred according to the morphing map. Though the generated model later requires the fine anatomical adjustments from the MRI/CT images, it can have the same set of muscles as that in the whole-body human musculoskeletal model. The previous work showed some results from the motion captured data of a laboratory mouse. However, they are difficult to be quantitatively compared and analyzed with respect to the results of human. Usually, when comparing kinematic movements of two skeletal systems, the common coordinate systems for the two are necessary. In our case, it can be regarded as a kind of problem to find the posture of mouse corresponding to, for example, the human standing posture.

This paper proposes a method for finding the common coordinate systems (homologous postures) between the human and other mammalian skeletal systems. The estimation of homologous postures enables us to map the joint and muscular mechanical properties of another mammalian model onto the human musculoskeletal model. Similarly to the musculoskeletal morphing, the method relies on the hypothesis that the homology of bone geometry around joint system between the species indicates that of the mechanical functions of the joint. The method makes use of the two geometrical morphing maps of bones connected by a joint. The homologous postures can be determined by computing the orientation-invariant deformation tensor from the morphing maps in order to extract the offset of rotation between the human and mammalian joint coordinates. Unlike the morphing techniques for animal models in the field of computer graphics [13], the method finds the homologous postures between the two mammalian skeletal systems in a systematic way according to the homology of bone geometry. This paper demonstrates the results of the homologous postures between the human and mouse skeletal models. The paper also shows the pilot study on comparison between the two models by using the homologous postures: the comparison of range of joint movement and the comparison of the joint angles when the muscles relax. The validity of the proposed method as well as our hypothesis about the homology of bone geometry and joint system between the species are examined through the comparison.

II. RELATED WORKS

This research tries to build a methodology to transfer the experimental results of musculoskeletal analysis of laboratory animals to human as shown in Fig. 1. The proposed method in this paper as well as musculoskeletal morphing in our previous work are based on the morphing technique called Skeletal Subspace Deformation (SSD) which is commonly used for computer animation [14]. The deformation with SSD requires some number of relevant coordinate systems on the morphed model. In the musculoskeletal morphing, those coordinate systems are located on the anatomical landmarks of bone surface according to the Mechanostat Theory [15], [16]. The theory explains that the geometry of an animal bone is determined by stress applied to the bone, typically by stress caused by muscles and gravity. It indicates that the biomechanical functional points such as muscle attachment points are determined relation to the anatomical landmarks of bone surface. On a pair of corresponding bones of human and mouse, the corresponding anatomical landmarks are searched and determined to be used as the coordinate systems of SSD. It should be noted that the morphing methods for animal models [13] usually deform the skin surface directly to the another target in order to resemble the appearance. Our approach relies on the anatomical knowledge of the bone surfaces to map the biomechanical functional points.

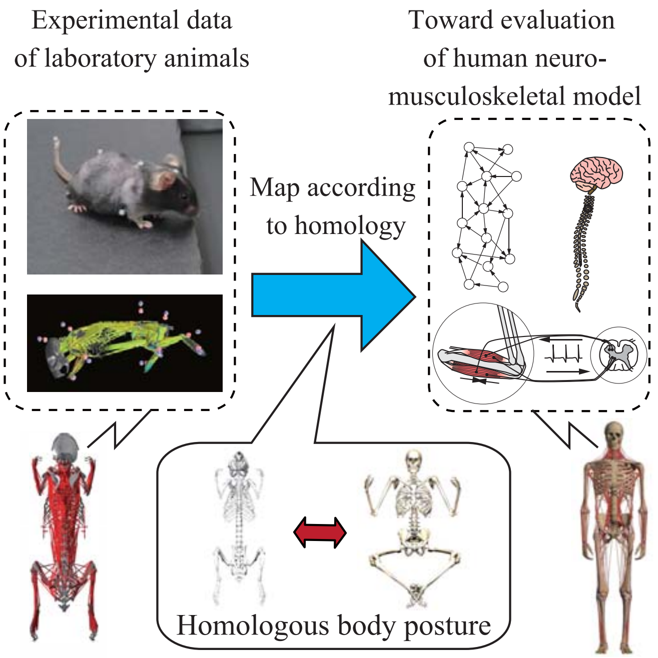

Fig. 1. Framework to transfer the knowledge from experiments of laboratory animals to the knowledge of human neuromusculoskeletal analysis

The musculoskeletal morphing just maps the skeletal system to the other in a different posture. Mapping the joint movements of human to those of mouse needs the correspondence between the human and mouse posture. In the field of computer graphics, the technology of transferring human movements to those of different characters is called motion retargeting [17]. It usually requires the morphing maps of the skeletal system between two characters. By using the morphing maps, the human motion data can be mapped onto different characters. This technology has been applied to generating the movements of a humanoid robot [18], [19]. In robotics applications, physical consistency and control issues are additionally considered in the morphing process.

In the above related methods, the homologous postures between the two models are predetermined in a heuristic way. The proposed method, on the other hand, automatically determines the homologous postures even if each skeletal system is in a different posture. The method also relies on the bone geometry information according to the Mechanostat Theory. In the proposed method, we hypothesize that the homology of joint mechanical properties between the two species; the geometric feature of two bones connected by a joint is determined in relation to the biomechanical functions of joint system. This hypothesis will be validated in section IV-B. Following the validation, the proposed method extracts the offset of joint orientation between the two species, by computing the rotation-invariant deformation generated by the bone morphing in the neighborhood of the joint system. This deformation can be regarded as the evolutionary change of joint mechanical properties between the two species.

III. INTERSPECIES RETARGETING OF HOMOLOGOUS BODY POSTURE

A. Skeletal morphing

This section presents the method for morphing the skeletal model A to that of model B [11]. Each skeletal model is composed of bones and each bone is geometrically modeled as a polygonal object.

The first step is to find a map from bone of model A to the corresponding bone of model B. In some cases, it may be difficult to find one-to-one correspondence due to the difference in skeletal geometry between the two. For example, in the case of mapping from human and mouse, the number of bones in coccyx and spine is different. In such a case, we had better consider mapping between bones with many-to-one or one-to-many correspondence. The missing components such as tail bones are not considered in the mapping, which must be discussed taking account of evolutionary morphology. Let us define the set of the pairs of corresponding bones as $\mathbb{B}$. A pair of bones is represented by an element of the set: $b \in \mathbb{B}$. In bone pair $s \in \mathbb{S}$, let the bone of model A be $a(s)$ and that of model B be $b(s)$.

The second process is to search for corresponding anatomical landmarks of bone geometry in bone pair $s \in \mathbb{S}$. According to the Mechanostat Theory, the homology of bone geometry is related to the homology of biomechanical function. The corresponding landmarks of human and mouse femur bone is shown in Fig. 2 as an example. We search and label the corresponding landmarks manually according to [20], [7]. Let the set of the pairs of corresponding landmarks in bones pair b be defined as $\mathbb{L}(s)$. A pair of corresponding landmarks in bone pair s is represented as $l \in \mathbb{L}(s)$. The coordinate system is determined on each anatomical landmark. The origin of the orientation is located on the landmark and the orientation is determined according to the local geometry information such as the curvature of bone surface.

The morphing from skeletal model A to B is performed by SSD [14]. In this paper, the coordinate system of each landmark is regarded as the skeletal frame used in SSD. The overview of the morphing is shown in Fig. 3. Let us define ${}^A\boldsymbol{p}_s \in \mathbb{R}^3$ as the position of arbitrary point in the neighborhood of the bone of model A. The point is morphed by SSD and the position after the morphing ${}^B\boldsymbol{p}_s \in \mathbb{R}^3$ can be computed as:

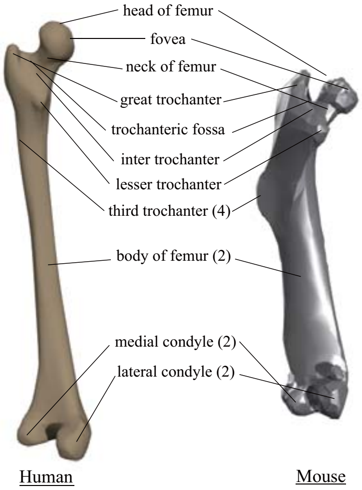

Fig. 2. Corresponding anatomical landmarks of left femur bone between human and mouse.

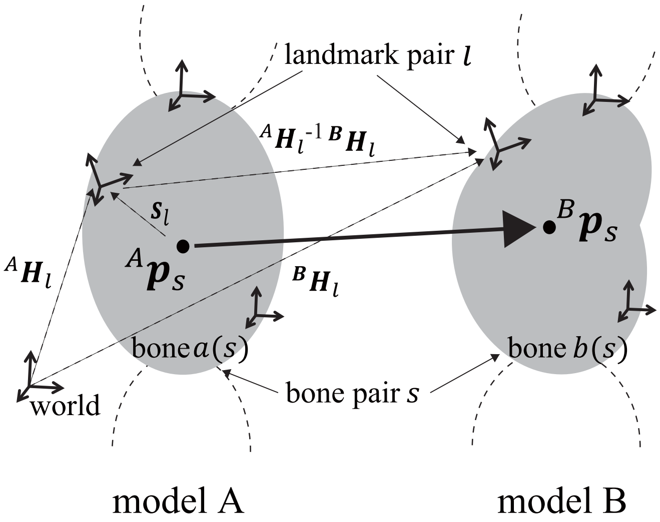

Fig. 3. Overview of skeletal morphing

$$\begin{bmatrix} {}^B\boldsymbol{p}_s \\ 1 \end{bmatrix} = \left\{ \sum_{l \in \mathbb{L}(s)} \omega_{s,l}({}^B\boldsymbol{p}_s)\,{}^A\boldsymbol{H}_l\,{}^B\boldsymbol{H}_l^{-1} \right\} \begin{bmatrix} {}^A\boldsymbol{p}_s \\ 1 \end{bmatrix} \tag{1}$$

where, ${}^*\boldsymbol{H}_i$ ($* = A\ or\ B$) is the homogeneous transformation matrix representing position ${}^*\widehat{\boldsymbol{p}}_i$ and orientation ${}^*\widehat{\boldsymbol{R}}_i$ of the coordinate system on the landmark of model A or B in pair $i \in \mathbb{L}(s)$:

$$ {}^*\boldsymbol{H}_i \triangleq \begin{bmatrix} {}^*\widehat{\boldsymbol{R}}_i & {}^*\widehat{\boldsymbol{p}}_i \\ \boldsymbol{O}_{1\times 3} & 1 \end{bmatrix} \tag{2}$$

The weighing function $\omega_{s,l}(\boldsymbol{p})$ is determined according to the followings:

$$\omega_{s,l}(\boldsymbol{p}) \triangleq \frac{s_l(\boldsymbol{p})}{\sum_{k \in \mathbb{L}(s)} s_k(\boldsymbol{p})} \tag{3}$$

$$s_k(\boldsymbol{p}) \triangleq \frac{1}{||\boldsymbol{p} - {}^A\widehat{\boldsymbol{p}}_k||^4 + \varepsilon} \tag{4}$$

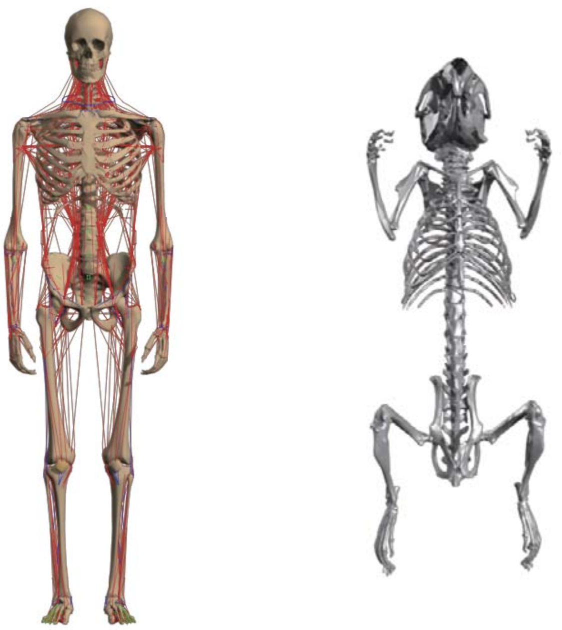

Fig. 4. Human musculoskeletal model (left) and mouse skeletal model (right)

Fig. 5. Morphed human skeletal model (left). By using the bone morphing maps, the musculotendinous models in the human model is mapped onto the mouse skeletal model (right).

where, ε is a small positive constant for preventing division by zero. The weighing function indicates the normalized value of the inverse of the cubed distance from the corresponding landmark.

After morphing with **eq.**(1) for all bone pairs ($\forall s \in \mathbb{S}$), the skeletal system of model A will be morphed to that of model B.

In our previous work, the skeletal model of human was morphed to that of mouse. The human musculoskeletal model [1] and the mouse skeletal model [12] are shown in the left and right of Fig. 4. The human skeletal model was transformed to the mouse by the skeletal morphing as shown in the left of Fig. 5. This result was used in order to map the muscular attachment points of the human musculoskeletal model onto the mouse skeletal model, as shown in the right of Fig. 5.

B. Joint posture retargeting based on continuum mechanics

The skeletal morphing consists of the several morphing maps between the bone pairs. Each map is designed according to the initial placement of bones. In Fig. 5, the human skeletal model at the standing posture is deformed to the mouse skeletal model at the different posture. It means that the skeletal morphing cannot separate the change of posture from the deformation. In many morphing or motion retargeting methods, the mapping between the two models is designed by making the posture of the one model similar to the other in advance. However, it is difficult to determine the homologous postures between the models with different morphologies. This section presents the method for computing the homologous postures between the two models by utilizing the morphing map of **eq.**(1).

In Mechanostat Theory, the bone geometry is determined by stress applied to the bone, for example, from joints or muscles. It indicates that the geometry of two bones around one joint is determined in relation to the joint mechanical system. We can place a hypothesis that the homology of bone geometry around a joint implies the mechanical function of the joint. If this hypothesis is correct, the mechanical relationship between the joint system of the animals can be extracted according to the two bone morphing maps around each joint. In general, the joint angle of the skeletal system means the relative orientation between the two bones connected by the joint. Let us separate the information of relative orientation from the two bone morphing maps.

In order to extract the relative coordinate information, we first compute the deformation around the neighborhood of the joint coordinate system. Let us simplify the expression of **eq.**(1) as follows:

$$ {}^{B}\boldsymbol{p}_s = \boldsymbol{W}_s({}^{A}\boldsymbol{p}_s){}^{A}\boldsymbol{p}_s \tag{5} $$

where,

$$ \boldsymbol{W}_s(\boldsymbol{p}) \triangleq \sum_{l\in\mathbb{L}(s)} \omega_{s,l}(\boldsymbol{p})\widehat{\boldsymbol{W}}_{s,l} \tag{6} $$

$$ \widehat{\boldsymbol{W}}_{s,l} \triangleq \boldsymbol{S}\,{}^{A}\boldsymbol{H}_l{}^{B}\boldsymbol{H}_l{}^{-1}\boldsymbol{S}^T \tag{7} $$

$$ \boldsymbol{S} \triangleq \begin{bmatrix}\boldsymbol{E}_3 & \boldsymbol{0}\end{bmatrix} \tag{8} $$

Matrix $\widehat{\boldsymbol{W}}_{s,l}$ does not depend on coordinate ${}^{A}\boldsymbol{p}_s$.

Let us compute the local displacement around position $\boldsymbol{p}$ by the morphing map determined by **eq**.(5). The deformation gradient tensor can be computed as:

$$ {}^{AB}\boldsymbol{F}_s \triangleq \frac{\partial^{B}\boldsymbol{p}_s}{\partial^{A}\boldsymbol{p}_s} = \boldsymbol{W}_s + \sum_{l\in\mathbb{L}(s)} \widehat{\boldsymbol{W}}_{s,l}{}^{A}\boldsymbol{p}_s \frac{\partial\omega_{s,l}}{\partial^{A}\boldsymbol{p}_s} \tag{9} $$

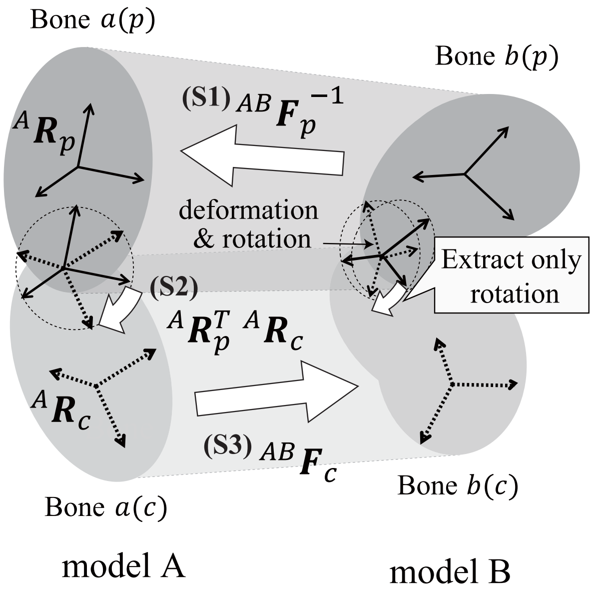

Fig. 6. Overview of joint coordinates mapping

where,

$$\frac{\partial \omega_{s,l}}{\partial^A \boldsymbol{p}_s} = \frac{1}{(\sum_{k\in\mathbb{L}(s)} s_k)}\frac{\partial s_l}{\partial^A \boldsymbol{p}_s} - \frac{s_l}{(\sum_{k\in\mathbb{L}(s)} s_k)^2}\left(\sum_{k\in\mathbb{L}(s)} \frac{\partial s_k}{\partial^A \boldsymbol{p}_s}\right) \tag{10}$$

$$\frac{\partial s_k}{\partial^A \boldsymbol{p}_s} = -\frac{4||^A\boldsymbol{p}_s - {}^A\widehat{\boldsymbol{p}}_k||^2}{(||^A\boldsymbol{p}_s - {}^A\widehat{\boldsymbol{p}}_k||^4 + \varepsilon)^2}({}^A\boldsymbol{p}_s - {}^A\widehat{\boldsymbol{p}}_k)^T \tag{11}$$

Let the skeletal multi-body system be modeled as a kinematic tree structure. Each joint is connected to the two bones: the root-side bone and the leaves-side bone. Let $p \in \mathbb{S}$ be the pair of root-side bones and $c \in \mathbb{S}$ be the pair of leaves-side bones. By using the morphing map of bone pair p and c, the corresponding deformation gradient tensors can be computed from **eq.**(9) and represented by ${}^{AB}\boldsymbol{F}_p$ and ${}^{AB}\boldsymbol{F}_c$, respectively.

Now we consider the composite mapping according to the following procedures.

(S1) Map the arbitrary joint coordinate of model *B* from the root-side bone of model *B* to the root-side bone of model *A* according to the inverse of bone morphing map of root-side bone pair *p*.

(S2) Map the resultant coordinate of model *A* from the root-side bone of model *A* to the leaves-side bone of model *A* according to the rotation of the joint of model *A*.

(S3) Map the coordinate of model *A* from the leaves-side bone of model *A* to the leaves-side bone of model *B* according to the bone morphing map of root-side bone pair *c*.

After the composite mapping, the deformation from the root-side bone to leaves-side on can be represented in the coordinate space of model *B*. The overview of the mapping is shown in Fig. 6. The deformation gradient tensor according to this mapping is computed as follows:

$${}^{B}\boldsymbol{F}_{pc} \triangleq {}^{AB}\boldsymbol{F}_p^{-1}({}^{A}\boldsymbol{R}_p{}^{T\,A}\boldsymbol{R}_c)^{AB}\boldsymbol{F}_c \tag{12}$$

The deformation gradient tensor is known to be decomposed into a product of two tensors:

$${}^{B}\boldsymbol{F}_{pc} = {}^{B}\boldsymbol{R}_{pc}{}^{B}\boldsymbol{U}_{pc} \tag{13}$$

where, ${}^{B}\boldsymbol{R}_{pc}$ indicates a rotation tensor and ${}^{B}\boldsymbol{U}_{pc}$ means a right stretch tensor. The tensor ${}^{B}\boldsymbol{U}_{pc}$ is positive definite and symmetric tensor. Since the pure rotation due to the above bone mapping corresponds to ${}^{B}\boldsymbol{R}_{pc}$, we now extract ${}^{B}\boldsymbol{R}_{pc}$ from ${}^{B}\boldsymbol{F}_{pc}$. The above separation of rotation and stretch is useful and reliable for large shape deformation and interpolation, and is often used in the field of computer graphics [21].

A well-known conventional method for stress analysis of a deformable object is to use the rotation-independent tensor of deformation such as the right Cauchy-Green tensor defined as:

$${}^{B}\boldsymbol{C}_{pc} \triangleq {}^{B}\boldsymbol{F}_{pc}{}^{T\,B}\boldsymbol{F}_{pc} = {}^{B}\boldsymbol{U}_{pc}^2 \tag{14}$$

The tensor ${}^{B}\boldsymbol{R}_{pc}$ can numerically be computed by using the singular value decomposition of ${}^{B}\boldsymbol{F}_{pc}$:

$${}^{B}\boldsymbol{F}_{pc} = \boldsymbol{SVD}^T \tag{15}$$

From **eq.**(13), **eq.**(14), and **eq.**(15), ${}^{B}\boldsymbol{R}_{pc}$ can be computed as:

$${}^{B}\boldsymbol{R}_{pc} = \boldsymbol{SD}^T \tag{16}$$

The tensor ${}^{B}\boldsymbol{R}_{pc}$ indicates the relative orientation around joint coordinate from the root-side bone to the leaves-side one of model *B*. By computing the difference of the corresponding relative orientation of model *A*, the difference of the joint posture between the two models can be computed as:

$$\delta\boldsymbol{R}_{pc} = \left({}^{A}\boldsymbol{R}_p{}^{T\,A}\boldsymbol{R}_c\right)^T {}^{B}\boldsymbol{R}_{pc} \tag{17}$$

The homologous joint posture of model *B* can be obtained by moving the joint coordinate to cancel the difference $\delta\boldsymbol{R}_{pc}$. By computing and canceling $\delta\boldsymbol{R}_{pc}$ for all joints from the root-link to leaves-side, the homologous posture of model *B* corresponding to the posture of model *A* can be obtained.

IV. RETARGETING RESULTS AND VALIDATIONS OF HOMOLOGOUS POSTURES

A. Homologous postures of human and mouse

The proposed method was tested to compute the homologous postures between the human skeletal model [1] and the mouse skeletal model [12], by using the same skeletal morphing maps of corresponding bones as shown in [11]. As already mentioned, those morphing maps were designed according to the anatomical landmarks on bone geometry. The morphed human skeletal system by using the maps is shown in Fig. 5.

This section introduces the two pairs of homologous postures. The initial posture of the human skeletal system is shown in the left of Fig. 7 and the corresponding posture of the mouse skeletal system is in the right of Fig. 7. The right figure in Fig. 8 shows the initial posture of the

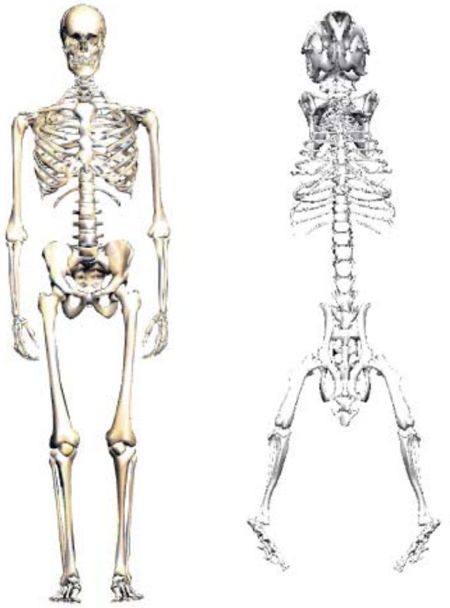

Fig. 7. Original human posture and corresponding mouse posture

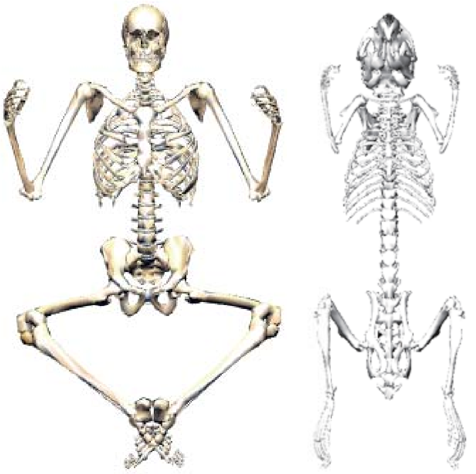

Fig. 8. Original mouse posture and corresponding human posture

mouse skeletal system and the left shows the corresponding posture of the human model. Even though those homologous postures show a difference of whole appearance, the local geometric features around each joint is in fact similar. For example, looking at the hip joint of each model in Fig. 9, the long axis along the femur bone in the neighborhood of the joint is perpendicular to the surface of the pelvis in each case. The comparison of the local geometric features around the joint will be detailed in the next subsection.

B. Analysis of range of joint movement

After computing the homologous postures, it is possible to directly compare the local geometric features between the skeletal system of different mammals. This section presents comparison of range of joint movement of the human and mouse skeletal systems, focusing on the analysis of the right hip joints. In the two skeletal models, the hip joints are modeled as spherical ones. Analysis of complex joints like shoulder or knee joints need to take into account combinational movements of rotation and translation. As a basic case here, let us consider the range of joint movement as the range where the two bones connected by the spherical joint can move without the collision between the geometric models of bones. It should be noted that the actual range of joint movement has additional constraints related to muscles, tendons and internal tissues.

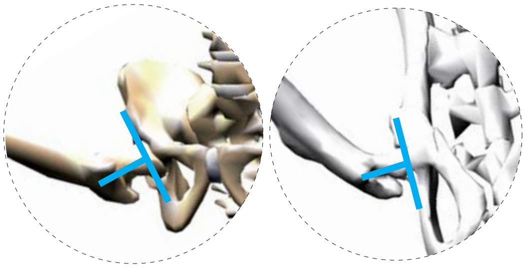

Fig. 9. Enlarged view of the right hip joint in Fig. 8

The range of flexion and adduction of the hip joint of the human skeletal model was examined by discretely changing each angle. The range was determined by the collision detection test [22] between the geometry model of right femur and that of pelvis. Each angle was changed in 6-degree increments from -180 to 180 degrees so that $61 \times 61 = 3721$ sets of flexion and adduction angle were checked by the collision detection test. At the same time as moving the human hip joint, the corresponding posture of the mouse model was also computed. The range of hip joint movement of the mouse model was also computed by the collision detection between its bone geometry models.

The results of the range of hip joint movement are shown in Fig. 10. The red cross marks indicate the infeasible range of movement of the human joint due to self-collision, and the blue circle marks mean that of the mouse joint. Those two regions in the figure exhibit high similarity. The center of the range of movement (i.e. white region in the figure) of the mouse joint is $(-14.4, -34.7)$ [deg] and that of the human joint is $(-9.3, -46.8)$ [deg]. The absolute error between the two is $(5.1, 12.1)$ [deg] which is almost within twice the resolution of discretized joint angles. This result indicates the validity of the computed homologous postures. The overlapped area of the regions is also evaluated. The total number of discretized sets of flexion and adduction angle is 3721. The 3308 sets show the same results of collision detection tests. The result shows 89% homology in the mechanical functions about the range of hip joint movement between the two species. The results of homology also provide the validity of the hypothesis in the method that the geometric shape of bones has a correlation to the mechanical functions of the joint.

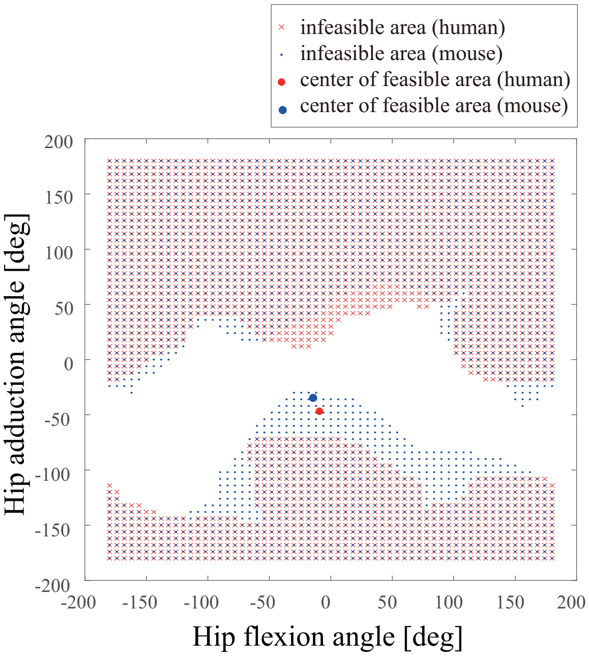

Fig. 10. Estimated motion range of two skeletal models

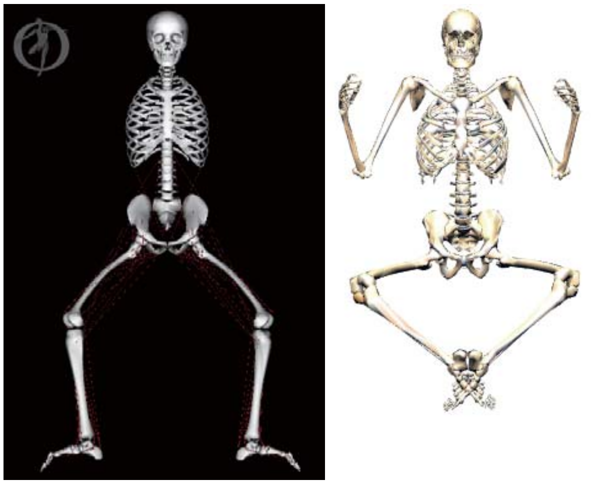

Fig. 11. Estimated human posture keeping neutral muscle lengths of OpenSim model (Left). The homogeneous posture of the human model in Fig. 8 is shown again for comparison purposes (Right).

C. Analysis of relaxed posture at neutral muscle length

Though our approach relies on the homology of bone geometry, the muscle architectural properties have several differences between the two spices as reported in [23]. This section presents a pilot study to compare the difference of the neutral postures of the musculoskeletal systems according to the common coordinate systems obtained from the proposed method. The neutral posture of the two models when all the muscles relax and are assumed to be at natural muscle length. The skeletal mode of the mouse in the right of Fig. 8 was developed by scanning the laboratory mouse frozen immediately after the mouse was killed. Since all the muscles of the mouse were almost relaxed, let us assume that the posture of the mouse in Fig. 8 corresponds to the neutral posture of the musculoskeletal system. On the other hand, the neutral posture of the human musculoskeletal system is difficult to be determined by human subject experiments. We therefore adopted the posture generated by using simulation software package called OpenSim [24] and its lower-body human model which includes the anatomical information of natural length of muscle models [25]. It should be noted that the skeletal model used in OpenSim is different from the model used to compute homologous postures. The correspondence between the two model was determined according to anatomical posture.

The neutral posture of the human model was computed by solving the optimization problem to minimize the sum of error from the natural length for all muscles in OpenSim. Each error is weighted by the maximum construction force of each muscle mode, resulting in the estimated posture shown in Fig. 11. Compared to the homologous posture in Fig. 11, the estimated one in Fig. 11 shows the similar orientation of the hip joint, whereas an apparent difference is observed at the knee joints. Since the knee joint was modeled by a spherical joint in the morphing process, it requires more detailed discussion, which will be addressed in our future investigations. The hip flexion and adduction angles of the human model with the neutral posture shown in Fig. 11 are $(37, -34)$ [deg]. The angles of the human model with the homologous posture corresponding to the neutral posture of the mouse model shown in Fig. 8 are $(75, -37)$ [deg]. While the results of the abduction angle show similar values, the flexion angle of the homologous posture in Fig. 8 is larger than that of the posture shown in Fig. 11. This result suggests that the difference between a biped and a quadruped produces different muscle development around the hip joint between the two species. It is therefore rational that the flexion angle in the case of the quadruped (mouse) was larger than that in the case of the biped (human). Based on the above results, the proposed method is expected to provide a framework to evaluate and compare the musculoskeletal functions between the different species quantitatively. For example, the proposed framework can potentially contribute to further discussion on the relationship between locomotion and muscle development. The validity and accuracy of the proposed method need to be evaluated by the experiments using laboratory mice in our future work.

V. CONCLUSION

In this paper, we developed a methodology allowing quantitative comparison between the musculoskeletal system of human and that of laboratory animal by transferring the joint coordinate systems between the two skeletal models. Given two skeletal models, the method estimates the homologous posture for the two according to the anatomical landmarks of bone geometry. The homology of bone geometry between mammalian species implies that of biomechanical functions of musculoskeletal system. Relying on the homology, we developed automatically determine the homologous posture between the two models. In the method, the morphing maps from one bone of the human to one of the other animal is designed by using a pair of landmarks of corresponding bones. This method separates the rotational offset from the distortion by analyzing the rotational-invariant deformation resolving the distortion between the coordinates in the morphing maps. The proposed method automatically computes the homologous posture according to the homology of bone geometry without depending on heuristic matching often seen in other morphing techniques.

The homologous postures between the human and mouse skeletal models were computed by the proposed method. The range of flexion and abduction of the human hip joint was compared to that of the mouse joint whose coordinates are represented with respect to the homologous posture. The two ranges were highly overlapped and showed 89 [%] similarity. This result shows that there exists the homology also in the range of skeletal movement between human and mouse. It indicates the validity of the proposed method to determine the homologous postures according to bone geometry.

The homologous postures can provide an indicator to compare the mechanical properties between the different mammalian musculoskeletal systems. According to pilot study comparing the neutral posture of the hip joint with relaxed muscles around the joint, the neutral posture of the human was numerically determined by using the anatomical information about natural muscle length. As a result, the flexion angle of the human hip joint was 37 degrees and that of the mouse joint was 75 degrees, whereas there was only a small difference in the abduction angle. This difference can be explained by the difference of muscle development between a biped and a quadruped.

As mentioned earlier, the proposed method is expected to provide a methodology of quantitative musculoskeletal evaluation between the different species. The analysis of other species like monkeys will provide the validity of the proposed framework. The further analysis and the evaluation of the accuracy need to be conducted by experimental data of laboratory mice in future studies. The method utilizes the theory of continuum mechanics to compute the evolutionary deformation generated by bone morphing. The analysis of the virtual mechanical stress due to the evolutionary deformation will be a clue to clarify the driving force of evolutionary change of bone geometry from the view point of locomotion, which will be investigated in our future work.

REFERENCES

[1] Y. Nakamura, K. Yamane, K. Fujita, and I. Suzuki, “Somatosensory computation for man-machine interface from motion-capture data and musculoskeletal human model,” *IEEE Trans. on Robotics*, vol. 21, no. 1, pp. 58–66, 2005.

[2] S. L. Delp and J. P. Loan, “A computational framework for simulating and analyzing human and animal movement,” *IEEE Computing in Science and Engineering*, vol. 2, no. 5, pp. 46–55, 2000.

[3] A. Murai, K. Kurosaki, K. Yamane, and Y. Nakamura, “Musculoskeletal-see-through mirror: Computational modeling and algorithm for whole-body muscle activity visualization in real time.,” *Progress in Biophysics and Molecular Biology*, vol. 103, no. 2-3, pp. 310–317, 2010.

[4] M. Sreenivasa, K. Ayusawa, and Y. Nakamura, “Modeling and identification of a realistic spiking neural network and musculoskeletal model of the human arm, and an application to the stretch reflex,” *IEEE Trans. on Neural Systems and Rehabilitation Engineering*, vol. 24, no. 5, pp. 591–602, 2016.

[5] R. H. Waterson and et al., “Initial sequencing and comparative analysis of the mouse genome,” *Nature*, vol. 420(6915), pp. 520–562, 2002.

[6] “Mouse genome informatics,” http://www.informatics.jax.org/, 2010.

[7] I. Bab, C. Hajbi-Yonissi, Y. Gabet, and R. Muller, *Micro-Tomographic Atlas of the Mouse Skeleton*, Springer, 2007.

[8] S. Oota, K. Mekada, Y. Fujita, J. Humphpheries, K. Fukami-Kobayashi, Y. Obata, T. Rowe, and A. Yoshiki, “Four-dimensional quantitative analysis of the gait of mutant mice using coarse-grained motion capture,” in *Proc. of the Annual Int. Conf. of the IEEE Engineering in Medicine and Biology Society*, 2009, pp. 5227–5230.

[9] J. P. Charles, O. Cappellari, A. J. Spence, D.J. Wells, and J. R. Hutchinson, “Muscle moment arms and sensitivity analysis of a mouse hindlimb musculoskeletal model,” *J. of Anatomy*, vol. 229, no. 4, pp. 514–535, 2016.

[10] W.-L. Johnson, D.-L. Jindrich, R.-R. Roy, and V.-R. Edgerton, “A three-dimensional model of the rat hindlimb: musculoskeletal geometry and muscle moment arms,” *Journal of biomechanics*, vol. 41, pp. 610–619, 2008.

[11] Y. Nakamura, Y. Ikegami, A. Yoshimatsu, K. Ayusawa, H. Imagawa, and S. Oota, “Musculoskeletal morphing from human to mouse,” in *Proc. of the IUTAM Symposium on Human Body Dynamics*, 2011.

[12] S. Oota, A. Yoshiki, Y. Fujita, J. Humpheries, K. Fukami-Kobayashi, Y. Obata, T. Rowe, and Y. Nakamura, “Development of a coase-grained skeletal model of laboratory mouse and its application,” in *Proc. of 1st Int. Conf. on Applied Bionics and Biomechanics*, 2010.

[13] S. Zuffi, A. Kanazawa, D. Jacobs, and M. J. Black, “3D menagerie: Modeling the 3D shape and pose of animals,” in *IEEE Conf. on Computer Vision and Pattern Recognition*, 2017, pp. 5524–5532.

[14] J. P. Lewis, Matt Cordner, and Nickson Fong, “Pose space deformation: A unified approach to shape interpolation and skeleton-driven deformation,” in *Proc. of the 27th Annual Conf. on Computer Graphics and Interactive Techniques*, 2000, SIGGRAPH ’00, pp. 165–172.

[15] H. Roesler, “Some historical remarks on the theory of cancellous bone structure (wolff’s law),” *Mechanical Properties of Bone*, vol. 15, pp. 27–42, 1981.

[16] H. M. Frost, “Skeletal structural adaptations to mechanical usage (satmu): 1. redefining wolff’s law: the bone modeling problem,” *The Anatomical Record*, vol. 4, no. 226, pp. 403–413, 1990.

[17] M. Gleicher, “Retargetting motion to new characters,” in *Proc. of the 25th Annual Conf. on Computer Graphics and Interactive Techniques*, 1998, pp. 33–42.

[18] N.S. Pollard, J.K. Hodgins, M.J. Riley, and C.G. Atkeson, “Adapting human motion for the control of a humanoid robot,” in *Proc. of the IEEE Int. Conf. on Robotics and Automation*, 2002, pp. 1390–1397.

[19] K. Ayusawa and E. Yoshida, “Motion retargeting for humanoid robots based on simultaneous morphing parameter identification and motion optimization,” *IEEE Trans. on Robotics*, vol. 33, no. 6, pp. 1343–1357, 2017.

[20] Carmine D. C., *Anatomy A Regional Atlas of the Human Body*, Lippincott Williams & Wilkins, 2007.

[21] M. Alexa, D. Cohen-Or, and D. Levin, “As-rigid-as-possible shape interpolation,” in *Proc. of the 27th annual conf. on Computer graphics and interactive techniques*, 2000, pp. 157–164.

[22] G. V. D. Bergen, “Efficient collision detection of complex deformable models using aabb trees,” *Journal of Graphics Tools*, vol. 4, no. 2, pp. 1–13, 1997.

[23] M. A. Mathewson, M. A. Chapman, E. R. Hentzen, J. Friden, and R. L. Lieber, “Anatomical, architectural, and biochemical diversity of the murine forelimb muscles,” *J. of Anatomy*, vol. 221, no. 5, pp. 443–451, 2012.

[24] S. L. Delp, F. C. Anderson, A. S. Arnold, P. Loan, A. Habib, C. T. John, E. Guendelman, and D. G. Thelen, “Opensim: Open-source software to create and analyze dynamic simulations of movement,” *IEEE Trans. on Biomedical Engineering*, vol. 54, no. 11, pp. 1940–1950, 2007.

[25] T.-L. Wickiewicz, R.-R. Roy, P.-L. Powell, and V. R. Edgerton, “Muscle architectuie of the human lower limb,” *Clin. Orthop. Rei. Res.*, vol. 179, pp. 275–283, 1983.